JOURNAL OF GEOPHYSICAL RESEARCH, VOL. 112, D10S02, doi:10.1029/2006JD007589, 2007

A chemical ionization mass spectrometry technique for airborne measurements of ammonia

J. B. Nowak,[1,2] J. A. Neuman,[1,2] K. Kozai,[1,2,3] L. G. Huey,[4] D. J. Tanner,[4]
J. S. Holloway,[1,2] T. B. Ryerson,[2] G. J. Frost,[1,2] S. A. McKeen,[1,2] and F. C. Fehsenfeld[1,2]

Received 31 May 2006; revised 30 October 2006; accepted 9 November 2006; published 10 February 2007.

[1] A chemical ionization mass spectrometer (CIMS) utilizing protonated acetone dimer ion chemistry to measure gas-phase ammonia (NH_3) from the NOAA WP-3D aircraft is described. The average sensitivity determined from in-flight standard addition calibrations ranged from 2.6 to 5 ion counts s^{-1} $pptv^{-1}$, depending on flow conditions, for 1 MHz of reagent ion signal. The instrument time response was determined to be 5 s from the 2 e-folding signal decay time after removal of a standard addition calibration. The instrumental background varied from flight to flight ranging from 0.5 to 1.3 ppbv. The variability between successive background measurements ranged from 50 pptv to 100 pptv. Total uncertainty for the 5 s data was conservatively estimated to be ±(30% + 125 pptv). Two NH_3 sources were sampled during the New England Air Quality Study–Intercontinental Transport and Chemical Transformation (NEAQS-ITCT) 2004 campaign, one urban and one agricultural. During the 25 July flight, enhancements in NH_3 mixing ratios were coincident with enhancements in CO, NOx, and SO_2 mixing ratios downwind of New York City. The NH_3 mixing ratios in the urban outflow plume ranged from 0.4 to 1 ppbv, or enhancements of 0.2 to 0.8 ppbv above local background. During the 15 August flight, NH_3 mixing ratios were enhanced 0.3 to 0.45 ppbv above local background directly downwind of an agricultural area northeast of Atlanta, Georgia. The NH_3 CIMS instrument has shown the ability to measure sub-ppbv NH_3 levels at high time resolution from an aircraft.

Citation: Nowak, J. B., J. A. Neuman, K. Kozai, L. G. Huey, D. J. Tanner, J. S. Holloway, T. B. Ryerson, G. J. Frost, S. A. McKeen, and F. C. Fehsenfeld (2007), A chemical ionization mass spectrometry technique for airborne measurements of ammonia, *J. Geophys. Res.*, *112*, D10S02, doi:10.1029/2006JD007589.

1. Introduction

[2] Ammonia (NH_3) is the dominant gas-phase base in the troposphere. As a consequence NH_3 abundance influences aerosol nucleation and composition [*Ball et al.*, 1999; *Gaydos et al.*, 2005; *Hanson and Eisele*, 2002; *McMurry et al.*, 2005; *Weber et al.*, 1998] and affects regional air quality, atmospheric visibility, and acid deposition patterns [*ApSimon et al.*, 1987; *Erisman and Schaap*, 2004]. Major sources of NH_3 to the troposphere include biomass burning and anthropogenic emissions from livestock waste, large-scale application of fertilizer, and automobile emissions [*Dentener and Crutzen*, 1994; *Schlesinger and Hartley*, 1992; *Fraser and Cass*, 1998; *Kean et al.*, 2000; *Moeckli et al.*, 1996; *Perrino et al.*, 2002]. Despite its importance, there are few observations of NH_3 above the planetary boundary layer. Some of the earliest were by filter or denuder techniques that required sampling times (>15 min) that are not well suited to aircraft traveling at speeds of 100 m s^{-1} or greater [*LeBel et al.*, 1985; *Alkezweeny et al.*, 1986]. NH_3 observations in concentrated plumes from biomass burning sources, where NH_3 mixing ratios are typically greater than 10 ppbv, have been reported [*Hurst et al.*, 1994; *Yokelson et al.*, 1999, 2003a; *Goode et al.*, 2000; *Sinha et al.*, 2003]. However, NH_3 mixing ratios as low as 0.1 ppbv have been hypothesized to influence important atmospheric processes, such as new particle formation [e.g., *Gaydos et al.*, 2005]. A sensitive and fast time resolution technique has been used in a ground study to examine urban NH_3 emissions [*Li et al.*, 2006]. However, to further understand the distribution of NH_3 throughout the atmosphere, its role in atmospheric processes such as aerosol formation, and the impact of anthropogenic and agricultural NH_3 sources on regional air quality, fast time resolution, sub-ppbv airborne observations are needed.

[3] This paper describes a new airborne chemical ionization mass spectrometer (CIMS) instrument used to measure NH_3 from the National Oceanic and Atmospheric Admin-

[1]Cooperative Institute for Research in Environmental Sciences, University of Colorado, Boulder, Colorado, USA.
[2]Chemical Sciences Division, Earth System Research Laboratory, NOAA, Boulder, Colorado, USA.
[3]Now at Department of Mathematics, Harvey Mudd College, Claremont, California, USA.
[4]School of Earth and Atmospheric Sciences, Georgia Institute of Technology, Atlanta, Georgia, USA.

0148-0227/07/2006JD007589$09.00

istration (NOAA) WP-3D aircraft during the New England Air Quality Study–Intercontinental Transport and Chemical Transformation (NEAQS-ITCT) study in July and August 2004 [*Fehsenfeld et al.*, 2006]. In this paper we describe the inlet, flow tube reactor, calibration system, and ion-molecule reaction scheme. The instrument detection sensitivity, precision, and time response are characterized using flight data. Lastly, the utility of these NH_3 observations is demonstrated by examining two plumes, one urban and one agricultural, sampled during NEAQS-ITCT 2004.

2. Instrument Description

[4] Various types of chemical ionization techniques have been used to measure atmospheric trace gases [*Clemitshaw*, 2004; *de Gouw and Warneke*, 2006; *Huey*, 2006, and references therein]. CIMS techniques use ion-molecule reactions to selectively ionize and detect trace species of interest in ambient air. This airborne NH_3 instrument (Figure 1) was developed from an aircraft nitric acid (HNO_3) CIMS instrument [*Neuman et al.*, 2002] and two ground-based NH_3 CIMS instruments [*Fehsenfeld et al.*, 2002; *Nowak et al.*, 2006]. The inlet, low-pressure flow tube reactor, and quadrupole mass spectrometer are similar to the airborne HNO_3 instrument described by *Neuman et al.* [2002]. However, the ion chemistry and instrument background determination are different than previously used in the ground-based NH_3 CIMS instruments. Other modifications include the addition of a collisional dissociation chamber (CDC) and an octopole ion guide [*Tanner et al.*, 1997; *Slusher et al.*, 2004]. The inlet delivers ambient air to a low-pressure flow tube reactor, where ions are produced to selectively cluster with NH_3. The ions are passed through the CDC where water clusters are broken off the parent ions. Finally, the ions are guided through the vacuum chamber by an octopole ion guide into a quadrupole mass spectrometer, where they are filtered and detected with an electron multiplier.

2.1. Inlet

[5] Fast time resolution measurements of traces gases, like NH_3 and HNO_3, are difficult because these gases readily adsorb and/or desorb from surfaces [*Neuman et al.*, 1999; *Yokelson et al.*, 2003b]. Laboratory tests similar to those described in the work of *Neuman et al.* [1999] were performed to determine the most appropriate inlet material. Other NH_3 instruments have used glass, Teflon, and halocarbon wax-coated steel inlets [*Owens et al.*, 1999; *Fehsenfeld et al.*, 2002; *Yokelson et al.*, 2003b]. Inlet materials tested in this study were tetrafluoroethylene (TFE) Teflon, fluorinated ethylene-propylene (FEP) Teflon, perfluoro-alkoxy (PFA) Teflon, polyvinylidene fluoride (PVDF), 6061 aluminum, 304 stainless steel, Dekabon 1300, borosilicate glass, nylon 6, and nylon 11. The sample inlet tubes were cut to a length of 0.34 m with internal diameters ranging from 3 to 5 mm. All tubes were cleaned by flushing with distilled water, followed by ethanol, and then purged with clean, dry N_2. For these experiments the total flow through the sample inlets was 3.5 standard liter per minute (slpm) of N_2 and the resulting Reynolds numbers (Re) ranged from 1550 to 1940, which are in the laminar flow regime. The calculated sample residence time in these sample inlets varied according to internal diameter and was no greater than 82 ms. 8 ppbv of NH_3 in clean, dry N_2 supplied by the blow off from a liquid N_2 dewar was sampled through each inlet tube at room temperature ($\sim$20°C) and the NH_3 signal rise, and subsequent decay after removal, were monitored similar to the method described by *Neuman et al.* [1999]. Additional experiments with the FEP, PFA, stainless steel, and glass inlet tubes were performed at high RH (72%) and at high RH with the inlet tubes heated to 40°C. Similar to the results given by *Yokelson et al.* [2003b], NH_3 exhibited an unacceptably large loss on the uncoated metal materials tested and therefore metal inlets were not subjected to further tests. FEP, PFA, and glass were all found to be acceptable, with 2 e-folding signal decay times ranging from 6 to 12 s, and PFA was chosen for the inlet used in the flight instrument. Proper sample tube handling and care were shown to be equally as important as selecting the proper tube material. Experiments designed to simulate the conditions of an aircraft mission (i.e., running, sitting idle overnight, running the next day, etc.) showed that the rise/decay characteristics were reproducible for a given inlet material only when a flow of clean, dry N_2 was used to purge the inlet during periods of instrument inactivity. This suggests that for sampling NH_3 an inlet time response determined in the laboratory with clean air may not be applicable to data collected in the field. If achieving a specific time response is necessary for a particular analysis, then for NH_3 sampling the time response for that instrument should be determined using ambient, field data. Therefore the time response of the inlet and CIMS instrument described in this paper was determined using ambient aircraft data obtained in flight throughout the entire field program (section 3.2).

[6] The sampling inlet is similar to that used for airborne HNO_3 measurements [*Neuman et al.*, 2002; *Neuman et al.*, 2003b]. The inlet is housed inside streamlined tubing that is mounted to a window plate of the aircraft and extends 0.33 m beyond the aircraft fuselage in order to sample outside of the aircraft boundary layer. Sampling was performed perpendicular to the direction of flight, and in this orientation is likely to discriminate against some of the large-diameter aerosol mass [*Ryerson et al.*, 1999]. All wetted sample line components were made from PFA Teflon. To minimize the effect of temperature fluctuations on the adsorption/desorption of NH_3 to the inlet walls, the inlet tubing was contained in an aluminum (Al) housing and thermostated at 30°C, which was determined to be the lowest controllable temperature for the typical aircraft cabin conditions encountered in flight during the NEAQS-ITCT mission. Previous field mission data showed negligible ammonium nitrate volatilization in a similar inlet using similar flow rates and thermostated at 50°C [*Neuman et al.*, 2003b]. The distance from the inlet tip to the flow tube reactor entrance was 0.55 m.

[7] Ambient air was brought in through one of two ports (Figure 1). One port was used for sampling ambient NH_3 while the second port was used for determining the instrument background by delivering air through a scrubber that removed NH_3 from ambient air. A heated PFA rotor valve located 0.11 m from the inlet tip was actuated pneumatically to switch the ambient airflow between the two ports. During ambient NH_3 measurements, ambient air was drawn through

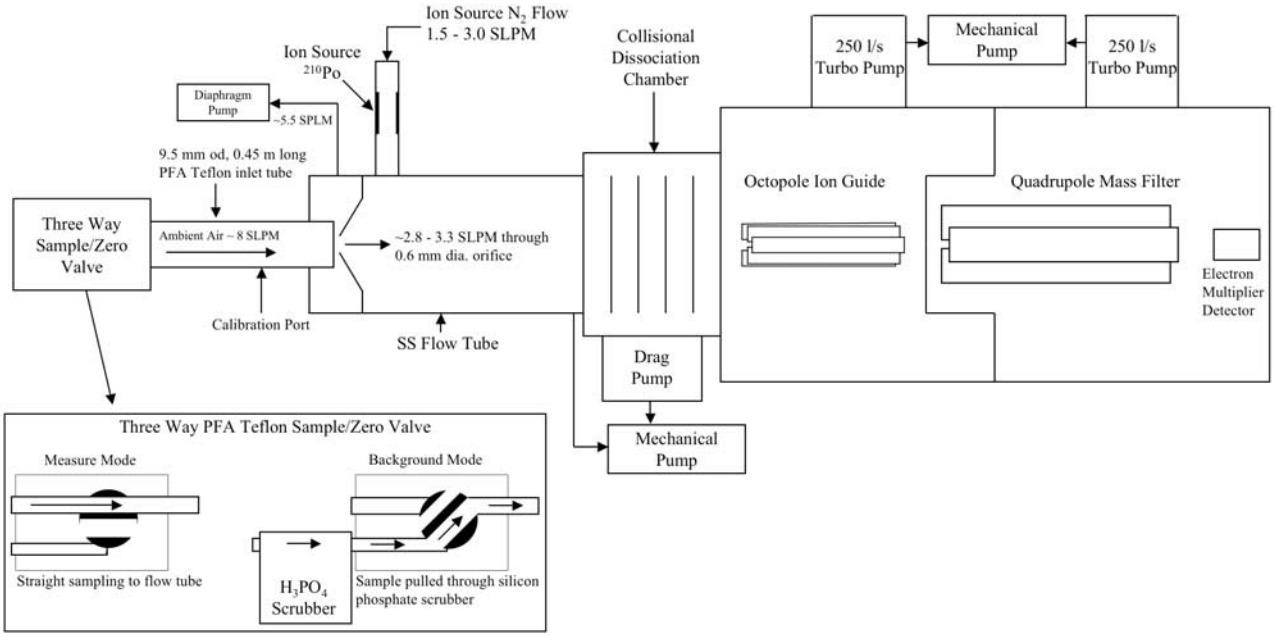

Figure 1. NH_3 CIMS instrument schematic.

a short section of PFA tubing (0.11 m length, 4 mm ID) and directly through the rotor valve. When the rotor valve was actuated, ambient air was diverted into an Al housing containing silicon phosphates (Perma Pure, Inc.) that form phosphoric acid when exposed to ambient levels of humidity, thereby removing NH_3 from ambient air. The Al housing (0.14 m length, 40 mm ID) was kept at 40°C to prevent water from condensing onto the scrubbing material. The NH_3 scrubber could not fit into the streamlined tubing housing the inlet, so it was mounted in the cabin on the window plate. When the instrument was in zero mode, ambient air was sampled by this second port through the scrubber, then through a 0.35 m length of 4 mm ID copper tubing, which extended the length of the winglet, and finally delivered to the rotor valve at the head of the inlet. Metal tubing was used to minimize cabin air NH_3 permeating into the zero line between the scrubber exit and the rotor valve. The exit of the PFA rotor valve connected to a PFA tube (0.45 m length, 8 mm ID) housed in a thermostated (30°C) Al tube that delivered ambient air to the entrance of the flow tube reactor. A rotary vane pump connected to the exit of the flow tube drew approximately 2.8 slpm through the inlet and flow tube. An additional flow of 5.2 slpm of air was maintained in the inlet with a diaphragm pump. The magnitude of this additional flow was chosen to minimize inlet residence time while maintaining laminar flow conditions. During NEAQS-ITCT at an altitude of 1000 m, the total inlet flow was 8 slpm and the inlet residence time was approximately 190 ms. To reduce NH_3 contamination of the instrument, an overflow purge of 100 sccm of N_2 was delivered continuously through the inlet via a critical orifice when the instrument was shut down between flights.

2.2. Flow Tube and Quadrupole Mass Spectrometer

[8] NH_3 is detected using ion-molecule reactions that occur in a low-pressure flow tube reactor where ambient air is mixed with ions produced in a radioactive ion source. Approximately 2.8 slpm of ambient air enters the flow tube through an Al sampling cone with a 0.6 mm diameter hole at the apex. Reagent ions enter the flow tube perpendicular to the ambient airflow through a port located 30 mm downstream from the Al sampling cone. The stainless steel flow tube (0.45 m long, 35 mm ID) was kept at approximately 10 V relative to the aircraft ground. The protonated acetone dimer ($(C_3H_6O)H^+(C_3H_6O)$) reagent ions are produced by typically flowing 3.5 slpm of N_2 with approximately 1 sccm from a cylinder containing 100 psi of N_2 doped with a mixture of 100 Torr of acetone (C_3H_6O) and 3 Torr of sulfur hexafloride (SF_6) over a 20 mCi ^{210}Po radioactive source. These ions react selectively and sensitively with NH_3 [*Fehsenfeld et al.*, 2002]. SF_6 was added to attach electrons in order to slow recombination and ambipolar diffusion losses of the positive ions and to increase total ion signal.

[9] One complication observed in the previous ground-based CIMS NH_3 measurements described by *Fehsenfeld et al.* [2002] using this ion chemistry is the tendency of $(C_3H_6O)H^+(C_3H_6O)$ and $(C_3H_6O)H^+(C_3H_6O)\bullet NH_3$ to further cluster with water in the low-pressure flow tube reactor. Additional water clustering distributes the reagent and product ions over multiple masses, thereby reducing the signal at any single mass and requiring additional masses to be monitored during a measurement cycle. This clustering also adds difficulty in interpreting the mass spectrum. To avoid these difficulties a CDC was used to break up water clusters downstream of the flow tube [*Tanner et al.*, 1997]. After exiting the low-pressure flow tube, the ions are then accelerated through the CDC via an electric field of approximately 1.5 V mm^{-1}. The CDC is maintained at <0.4 Torr with a molecular drag pump. Collisions inside the CDC dissociated weakly bound clusters such as $(C_3H_6O)H^+(C_3H_6O)\bullet(H_2O)_n$ and $(C_3H_6O)H^+(C_3H_6O)\bullet NH_3\bullet(H_2O)_n$ into the core cluster ions, simplifying the mass spectrum.

[10] The flat plate ion lenses used in both the HNO_3 system and the previous NH_3 ground system [*Fehsenfeld et al.*, 2002; *Neuman et al.*, 2002] were replaced with an octopole ion guide [*Hagg and Szabo*, 1986; *Slusher et al.*, 2004]. After leaving the CDC the ions are guided through the vacuum system by the octopole ion guide and into the quadrupole mass spectrometer, where they are filtered and detected with an electron multiplier. The combination of the CDC and octopole ion guide increased ion throughput, as measured by the acetone dimer signal, by an order of magnitude over the NH_3 ground system [*Fehsenfeld et al.*, 2002], and resulted in reagent ion signals over 1×10^6 counts s^{-1} (1 MHz) during the airborne study.

[11] The residence time in the flow tube depends on ambient airflow into the flow tube through the Al sampling cone, total flow through the radioactive source region, and the flow tube pressure. The ambient airflow through the sampling cone into the flow tube was not actively controlled and changed as a function of aircraft altitude. For the 0.6 mm diameter hole used, the flow through the orifice varied from 2.8 slpm at sea level down to 1.2 slpm at 6.4 km altitude. The flow through the ion source was controlled at either 1.5 or 3.5 slpm. The flow tube pressure ranged from 18 to 22 Torr. The calculated flow tube residence time was between 95 and 160 ms depending on the flow and pressure conditions.

2.3. Standard Addition Calibrations

[12] Standard addition calibrations were performed in-flight to track changes in the sensitivity of the CIMS instrument. The instrument was calibrated autonomously with minimal disruption of gas flow through the calibration source or inlet. Standard addition calibrations were performed at least hourly with the output of an NH_3 permeation device (Kin-tek, La Marque, Texas). The permeation device is housed in a temperature controlled PFA sleeve at 40°C. 45 sccm of N_2 continuously flows over the permeation device and through the PFA sleeve. A temperature-controlled crimp at the exit of the calibration system maintains the pressure in the sleeve at ~2 atm to reduce pressure changes in the calibration system in order to ensure stable output of NH_3 during flight [*Talbot et al.*, 1997].

[13] The output from the permeation device connects to a PFA tee located at the inlet. A vacuum line connects through a solenoid valve to the third leg of the tee. Calibration gas and some ambient air are removed in a 100 sccm flow through the vacuum line. This prevents the continuously flowing calibration gas from being introduced into the inlet when the solenoid is open during ambient measurements [*Ryerson et al.*, 1999]. When the solenoid valve closes, the calibration gas is added to the inlet. The resulting signal enhancement from a known amount of NH_3 is used to determine instrument sensitivity and time response.

[14] The stability of the permeation device was maintained between flights by removing the permeation oven from the aircraft and connecting it to a ground support system where the same flow and temperature conditions were maintained. Here the output of the NH_3 permeation device was measured by UV absorption at 184.95 nm between each flight [*Neuman et al.*, 2003a]. The average permeation rate showed no systematic change throughout the campaign and was 16 ± 0.3 ng min^{-1} with an estimated uncertainty of ±15%. This agreed within the estimated uncertainties with both the manufacturer's determination by weight loss (15 ng/min) and previous ion chromatography analysis (14.8 ng/min) for this permeation device. Additional laboratory tests show that, similar to a HNO_3 permeation tube [*Neuman et al.*, 2003a], the NH_3 permeation device output reproducibly returns to equilibrium in less than 2 hours after a short (<10 min) disruption in flow or temperature control. A 3 hour preflight period was provided during NEAQS-ITCT to allow the permeation device to equilibrate after it was installed on the aircraft, so in-flight calibrations were not affected by these perturbations.

3. Instrument Performance

[15] Instrument performance is assessed by examining instrument sensitivity, background signal, time response, and other in-flight diagnostics. From these performance criteria the accuracy, precision, and overall estimated uncertainty of the measurements are determined.

3.1. Ion Chemistry and Detection Sensitivity

[16] The protonated acetone dimer $(C_3H_6O)H^+(C_3H_6O)$ reacts sensitively and selectively with NH_3 to form a stable cluster ion, $(C_3H_6O)H^+(C_3H_6O)\bullet NH_3$ [*Fehsenfeld et al.*, 2002]. Similarly, protonated ethanol cluster ions also react sensitively and selectively with NH_3 [*Nowak et al.*, 2002, 2006]. However, in laboratory testing of the low-pressure flow tube setup used on the aircraft, it was found that sampling the liquid ethanol headspace described in the work of *Nowak et al.* [2002, 2006] was more prone to NH_3 contamination than the acetone/SF_6/N_2 gas bottle mixture. Therefore the protonated acetone dimer ion chemistry was used in the flight instrument. The major peaks seen in an ambient mass spectrum (Figure 2) are $(C_3H_6O)H^+(C_3H_6O)$, $(C_3H_6O)H^+(C_3H_6O)\bullet NH_3$, and their isotopes. The use of a CDC eliminates the H_2O clusters described in the work of *Fehsenfeld et al.* [2002], greatly improving the sensitivity and selectivity of the ion chemistry. NH_3 mixing ratios are determined by normalizing the product ion cluster signal, $(C_3H_6O)H^+(C_3H_6O)\bullet NH_3$, to the reagent ion signal $(C_3H_6O)H^+(C_3H_6O)$. Normalization accounts for changes that occur in the reagent signal over time since the product ion signal is linearly proportional to that of the reagent ion. While the reagent ion signal typically varied less than 30% over a single flight, the signal ranged from 1 to 3×10^6 counts/s (1–3 MHz) over multiple flights, depending on flow conditions and voltage settings.

[17] The sensitivity was determined from the response to in-flight standard addition calibrations. Standard addition calibrations of 2.3 to 2.7 parts per billion by volume (ppbv) were performed 5 to 7 times each flight with the output of the NH_3 permeation device in ambient air or ambient air scrubbed of NH_3. No consistent difference in detection sensitivity was found between these cases. Each calibration was 2 min in duration (Figure 3) to allow calibration lines to equilibrate and assure that steady state had been reached, though on the basis of Figure 3 and the time response analysis (see section 3.2) this could likely be shortened in future studies. The average sensitivity ($\pm 1\sigma$) for each flight was determined by taking the normalized sensitivity and multiplying by the acetone dimer reagent ion count rate to

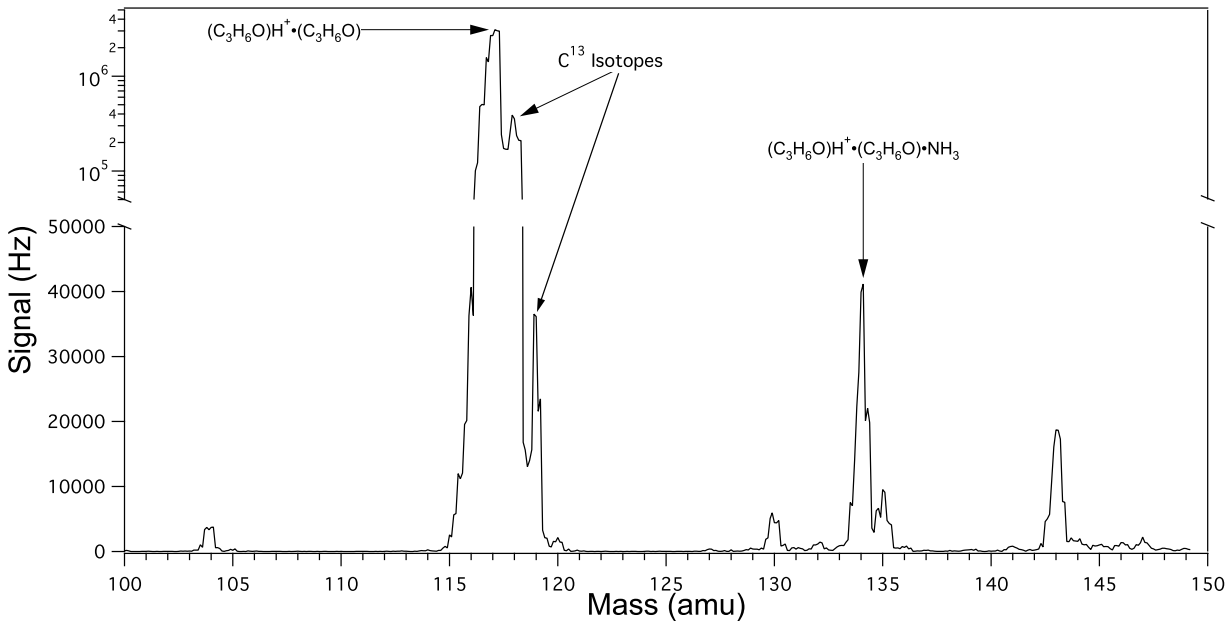

Figure 2. An ambient mass spectrum taken during the 9 July flight at 500 m altitude. The signal scale is linear under 50,000 Hz. The ambient NH_3 mixing ratio was 1.4 ppbv on a 1 ppbv background for this part of the flight.

account for reagent ion variability from flight to flight. For an ion source flow of 1.5 slpm, the average sensitivity was 5 ± 1.3 Hz/pptv for 1 MHz of reagent ion signal. At a higher ion source flow of 3.5 slpm, the average sensitivity dropped to 2.6 ± 0.5 Hz/pptv for 1 MHz of reagent ion signal. Two different ion source flows were used in an attempt to better understand the source(s) of the instrument background (section 3.3). Because the flow through the sampling cone

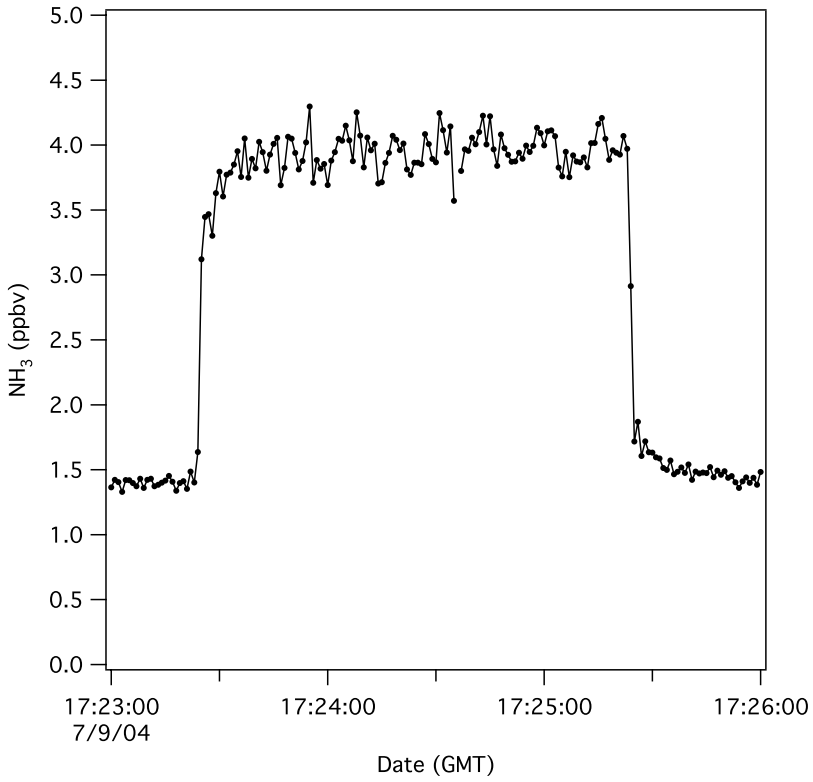

Figure 3. NH_3 mixing ratios during an ambient in-flight standard addition calibration at 1000 m altitude. The calibration mixing ratio was 2.6 ppbv and the background level was ~0.8 ppbv during the time period shown.

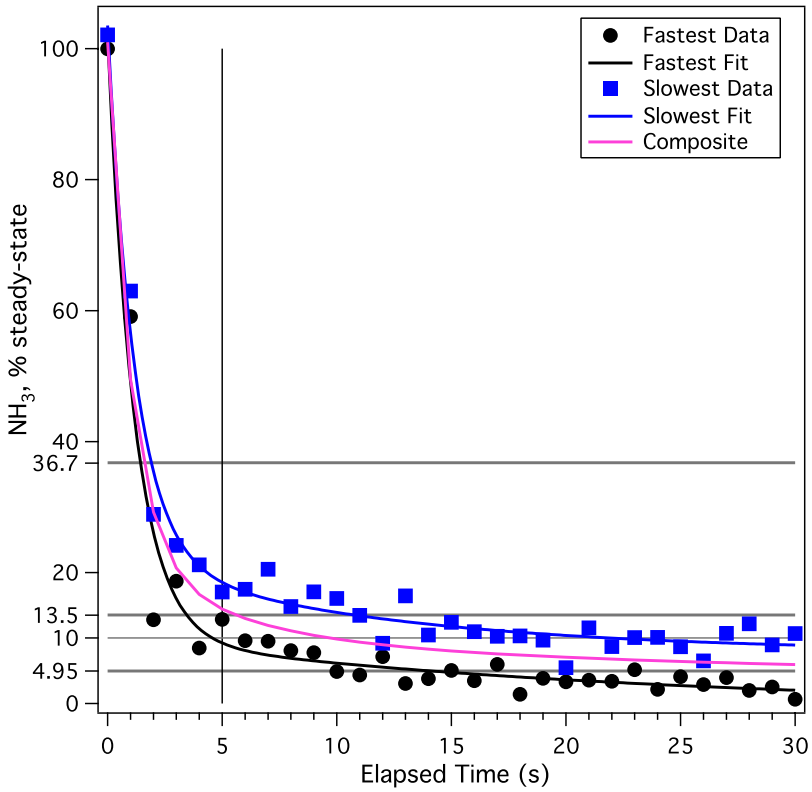

Figure 4. The 1 s data and fits for the fastest (black) and slowest (blue) signal steady state decay along with a composite (red) of all 60 of the fitted curves plotted against the time since calibration termination.

was not actively controlled, some of the sensitivity variability was likely due to changes in the total flow through the flow tube reactor at different altitudes. The sensitivity showed no dependence on ambient water vapor mixing ratios. Calibrations were performed at too few altitudes to determine if the sensitivity was altitude-dependent.

3.2. Time Response

[18] The NH_3 CIMS instrument collected data at a time resolution of 1 s. The 1 s data were used to determine the instrument time response and an appropriate averaging time. Each decay of the NH_3 signal following the removal of the calibration gas was fitted with a triple exponential decay curve, where the preexponential terms are expressed as a percentage of steady state calibration level and t is the time in seconds since the calibration was terminated, similar to the HNO_3 time response analysis by *Ryerson et al.* [1999, 2000]. Standard addition calibrations and the subsequent signal decays occurring during ascents or descents were excluded from this analysis. The 1 s data and fits for the fastest and slowest decay are shown in Figure 4, along with a composite of all the fitted curves (60 total). No correlation was found between any ambient condition, such as water vapor concentration or temperature, and decay time. From Figure 4, the 1 e-folding signal decay time for all the decay curves was 2 s or less. The 2 e-folding signal decay time ranged from 4 s to 10 s with that for the composite curve approximately 5 s. Since on average the 2 e-folding signal decay time was 5 s and for all cases at least 80% of the signal decay occurred within 5 s, 5 s was used as the observed instrument time response during NEAQS-ITCT 2004 and the data were archived as 5 s averages.

3.3. Instrument Precision and Uncertainty

[19] The background was determined in-flight by periodically pulling ambient air through a scrubber filled with commercially available silicon phosphates (Perma Pure, Inc.) and heated to 40°C to prevent water condensation [*Nowak et al.*, 2006]. The silicon phosphates reacted with ambient levels of humidity and formed phosphoric acid that scrubbed NH_3 from the ambient sample. The silicon phosphate scrubbing material was changed before every flight to prevent ammonium phosphates from building up and reducing the NH_3 scrubbing efficiency. The background is believed to come from either the desorption of NH_3 from inlet and/or ion-molecule reactor surfaces or from NH_3 contamination either in the N_2 used as the ion source flow gas or acetone/N_2 mixture used for generation of ions. The absolute background level varied from flight to flight and ranged from 0.5 ppbv to 1.3 ppbv. During a given flight the difference between consecutive backgrounds ranged from 50 pptv to 100 pptv. It is likely that the change in the absolute background level from flight to flight was due to differing levels of NH_3 contamination in the N_2 cylinders used to deliver the ion source and purge gas flows, or from exposure of supply lines to cabin air containing high levels of NH_3 during the exchange of empty N_2 cylinders.

[20] A 35 min ambient NH_3 time series showing a measurement/background sequence is shown in Figure 5. Both 1 s and 5 s average data are shown. The average background for the time period shown here is 1.1 ppbv.

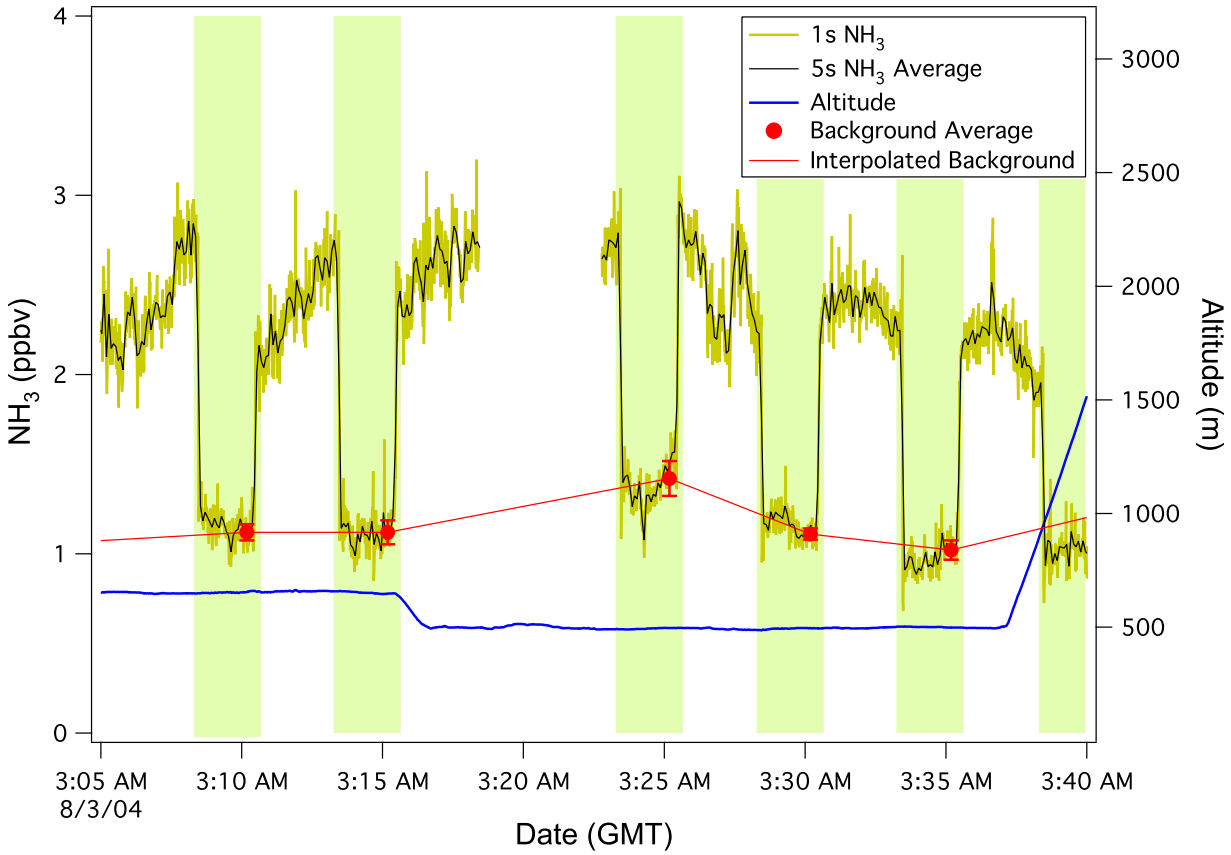

Figure 5. A 35 min NH_3 measurement sequence from the flight on 3 August. The shaded areas indicate the time periods the instrument was in background mode. The interpolated background is subtracted from the total signal to determine ambient levels. Shown are 1 s NH_3, 5 s NH_3 average, altitude, background average, and the interpolated background data.

Determination of the background allows the quantification of the actual instrument variability over time. This includes the uncertainty in each background and the difference between consecutive backgrounds. From the example shown here the 1 σ standard deviation on the backgrounds is 90 pptv for 1 s data and 45 pptv for 5 s averages, which are slightly larger than expected from counting statistics on the signals. The average difference between consecutive backgrounds was 100 pptv. So, for this example, an additional 110 pptv ($(45\ \text{pptv}^2 + 100\ \text{pptv}^2)^{1/2}$) was included into the uncertainty for the 5 s data. From the instrument performance criteria discussed here, the combined uncertainty for the instrument during NEAQS from calibration accuracy and background determination is estimated to range from ±(25% + 80 pptv) to ±(30% + 125 pptv) depending on the flight and operating conditions.

4. Field Observations and Discussion

[21] The 5 s data obtained during NEAQS-ITCT 2004 enabled observation of NH_3 in plumes from a variety of sources. Two examples described here, an urban plume downwind of New York, New York, and emissions from an agricultural source northeast of Atlanta, Georgia, are used to demonstrate the utility of this instrument. In addition to the NH_3 data, observations of carbon monoxide (CO), nitric oxide (NO), nitrogen dioxide (NO_2) and sulfur dioxide (SO_2) are used in this analysis. NO_2 and NO were measured by 2 separate channels of a chemiluminescence detector and were averaged to 1 s. NO_2 was measured with an uncertainty of ±(8% + 25 pptv) and NO was measured with an uncertainty of ±(5% + 10 pptv) [*Ryerson et al.*, 2000]. CO data were reported at 1 s intervals using a vacuum UV fluorescence instrument with an uncertainty of 5% and a 3 σ detection limit of 1.7 ppbv [*Holloway et al.*, 2000]. Sulfur dioxide (SO_2) measurements were made using a TECO 43C-TL pulsed fluorescence instrument that has been modified for aircraft operation with an estimated uncertainty of 15% and a 3 σ detection limit of 0.6 ppbv [*Ryerson et al.*, 1998]. The area and point source emissions data were taken from the Environmental Protection Agency (EPA) 1999 National Emissions Inventory (NEI99) version 3 as described in the work by *Frost et al.* [2006]. The NEI99 area emissions are presented on a 4 km resolution grid.

4.1. Urban Plume

[22] The New York metropolitan area is a significant NH_3 area source (Figure 6). In densely populated area with high vehicular traffic with no nearby agricultural activity, sources of NH_3 are believed to include vehicular emissions, waste disposal and recycling facilities, and power generation facilities using selective catalytic reduction (SCR) techniques to reduce NOx emissions [*Fraser and Cass*, 1998; *Kean et al.*, 2000; *Perrino et al.*, 2002; *Li et al.*, 2006]. The

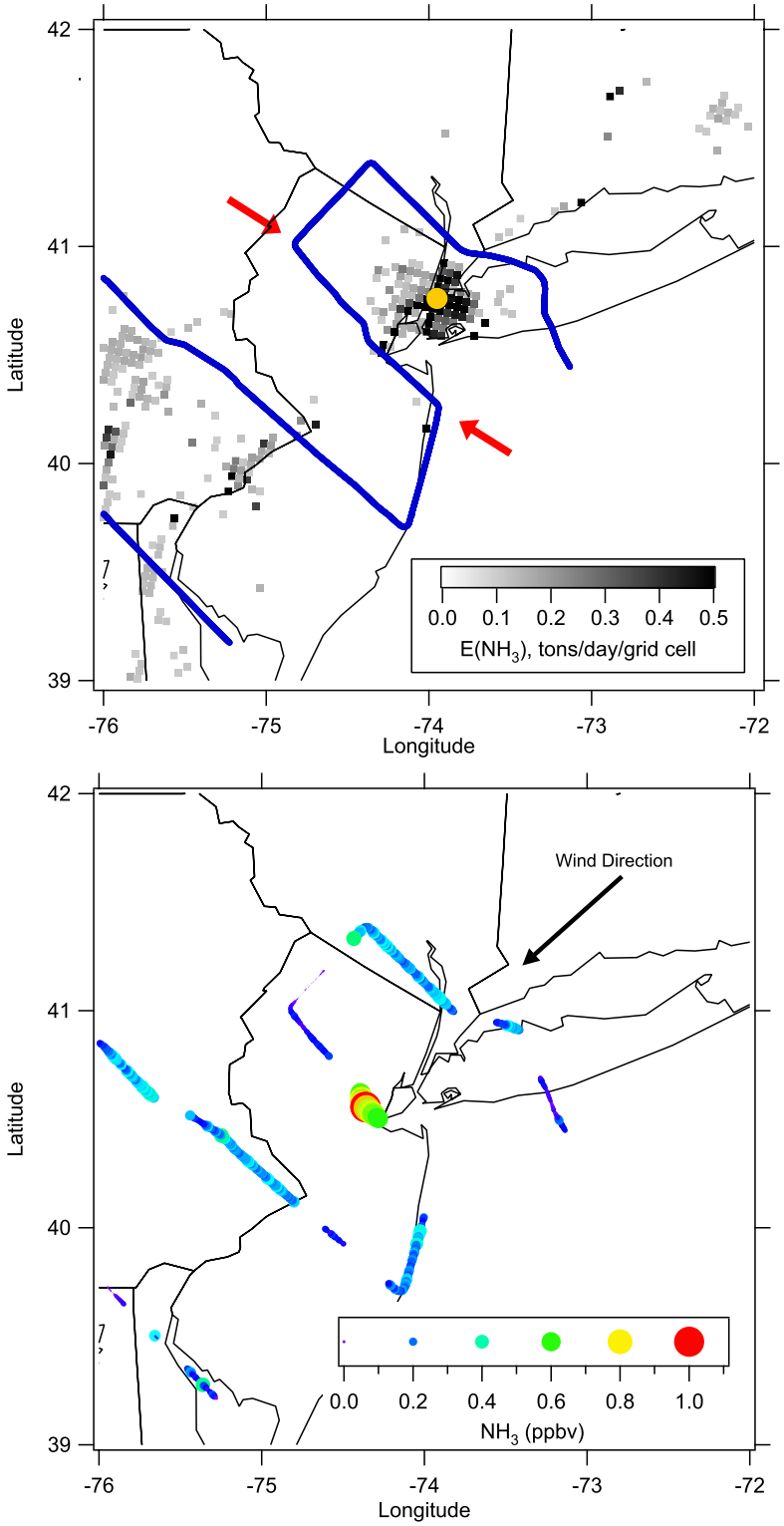

Figure 6. (top) WP-3D 25 July flight track for altitudes below 1.5 km superimposed on a map of NH_3 area emissions from the NEI99 on a 4 km resolution grid. Only NH_3 emissions greater than 0.1 tons/day/grid cell are shown. The yellow dot represents the 74th Street power facility, which is the largest NH_3 point source in New York City (518 tons/year). The flight leg indicated by the red arrows is shown in Figure 6 as a time series plot. (bottom) Same flight track shown colored and sized by NH_3 mixing ratios. The wind direction is indicated by the black arrow.

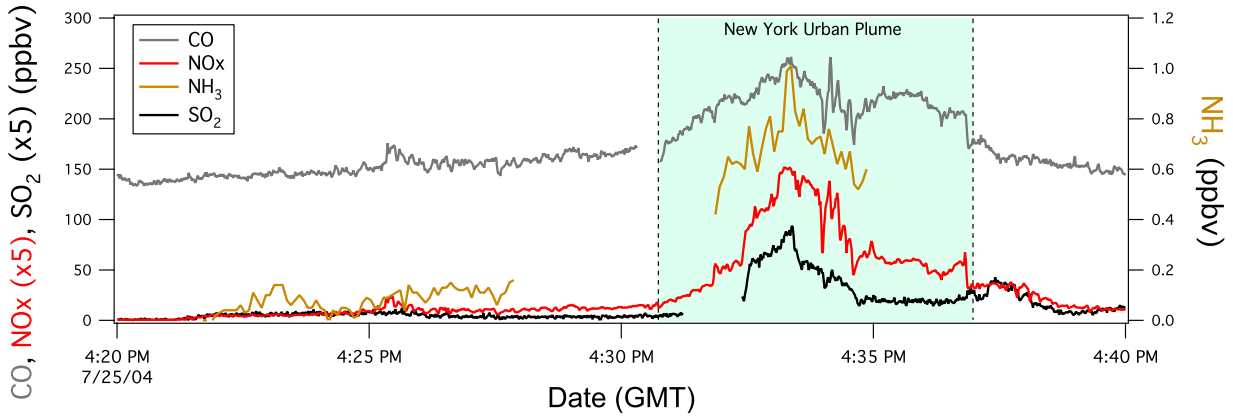

Figure 7. Time series of 1 s CO, NOx, SO_2 (left axis) and 5 s NH_3 (right axis) observations from the 25 July flight leg indicated by the black arrows in Figure 5. NOx and SO_2 mixing ratios have been multiplied by 5 for scaling purposes. The New York urban plume, as identified by the CO observations, is shaded.

25 July flight included sampling in this region. The flight track below 1.5 km is shown in Figure 6 (top) along with the New York City NH_3 area emissions and the location of the largest identified NH_3 point source in the city, the 74th Street power generation facility. In Figure 6 (bottom) the same flight track is shown colored and sized by the 5 s NH_3 observations. The gaps in the flight track and time series (discussed below) indicate the times of in-flight instrument diagnostics, such as background and calibration sequences or the scanning of a mass spectrum. With the wind coming out of the northeast, the section of the flight track indicated by the red arrows (Figure 6) was directly downwind of the metropolitan area at an altitude of approximately 500 m.

[23] The time series of the measurements made during the section of the flight track is shown in Figure 7. The shaded area corresponds to the urban outflow from New York. CO, NOx, and SO_2 mixing ratios were enhanced in this plume, reaching 260 ppbv, 30 ppbv, and 18 ppbv, respectively. The high levels of both SO_2 and CO indicate that power plant/industrial emissions were intermingled with vehicular emissions. NH_3 mixing ratios ranged from 0.4 to 1 ppbv in the New York City emission plume and were <0.15 ppbv outside of it. The structure observed in the NH_3 mixing ratios was correlated with enhancements observed in the NOx and CO mixing ratios. Identifying the exact locations of the NH_3 source(s) is uncertain, given the NH_3 data gaps. However, since little NH_3 enhancement was coincident with the slight CO enhancement observed during the flight leg across the middle of New Jersey (Figure 6), these observations suggest that gas-phase NH_3 was not readily transported beyond the source region. Since NH_3 can be lost from the gas-phase by surface deposition and particle formation or growth, more data are needed to understand the fate of these emissions and their regional impact.

4.2. Agricultural Plume

[24] Agricultural sources, such as fertilization and waste production from animal husbandry, also release large amounts of NH_3 into the atmosphere. The WP-3D transit flight on 15 August from Portsmouth, New Hampshire, to Tampa, Florida, included airborne sampling downwind of agricultural emission sources northeast of Atlanta, Georgia. Northeast of Atlanta is an area of concentrated poultry production, determined from the 2002 United States Department of Agriculture's Georgia state and county agricultural profiles available at http://www.nass.usda.gov/census/census02/profiles/ga/index.htm. The 15 August flight track below 1.5 km is shown in Figure 8 (top) along with the NH_3 area emissions of northern Georgia. The flight track skirted the edge of the agricultural NH_3 sources at altitudes between 750 and 800 m. In Figure 8 (bottom) the same flight track is shown colored and sized by the 5 s NH_3 observations with wind barbs of the 5 min average wind speed and direction.

[25] The highest NH_3 mixing ratios were observed on the legs directly downwind of and nearest to the agricultural area. On these legs CO, NOx, and SO_2 mixing ratios were low (120 ppbv, <1 ppbv, and <1 ppbv, respectively) and were not correlated with NH_3 mixing ratios that ranged from 0.5 to 0.65 ppbv, suggesting that these were truly agricultural and not vehicular or industrial emissions from upwind urban areas, such as Athens, Georgia. Further downwind from the source NH_3 levels dropped to less than 0.25 ppbv. NH_3 mixing ratios directly over Atlanta ranged from 0.3 to 0.4 ppbv, not reaching the levels observed downwind of New York City. Since the aircraft was unable to fly below a cloud deck over directly above Atlanta, the observed NH_3 mixing ratios were likely affected by inhibited vertical transport, cloud scavenging, and surface deposition. Thus not only the source strength but also local meteorological conditions need to be accounted for in the analysis of transport and the resulting distribution of NH_3 from surface sources.

5. Summary and Conclusions

[26] NH_3 was detected selectively and sensitively with a CIMS technique utilizing a protonated acetone dimer detection scheme aboard the NOAA WP-3D aircraft during the 2004 NEAQS-ITCT field campaign. The average sensitivity determined from in-flight standard addition calibrations ranged from 2.6 to 5 Hz/pptv for 1 MHz of reagent ion and could be adjusted by varying the flow tube residence time. The average 1σ variation in sensitivity for a given

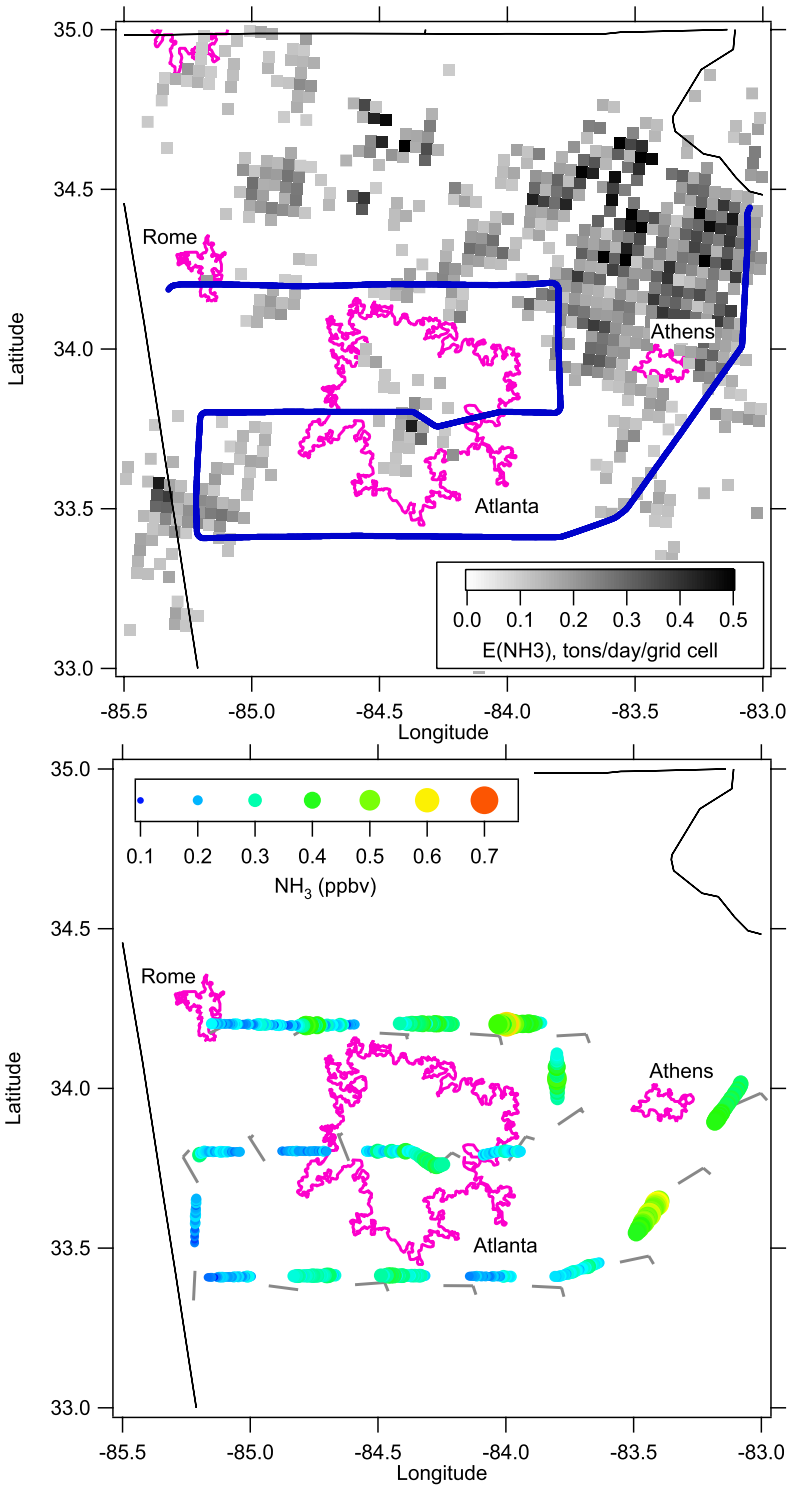

Figure 8. (top) WP-3D 15 August flight track for altitudes below 1.5 km superimposed on a map of northern Georgia NH_3 area emissions from the NEI99 on a 4 km resolution grid. Only NH_3 emissions greater than 0.1 tons/day/grid cell are shown. The urban areas of Rome, Athens, and Atlanta are also displayed. (bottom) Same flight track shown colored and sized by NH_3 mixing ratios along wind barbs of the 5 min average wind speed and direction. The wind barbs are slightly offset from the flight track for clarity.

flight was 20–25%. A heated/thermostated PFA inlet was used for sampling ambient air. The instrument time response was determined in flight from the NH_3 signal decay after removal of a standard addition calibration. The 2 e-folding signal decay time for all calibration curves analyzed ranged from 4 s to 10 s and on average was 5 s. This suggested the instrument time response was on the order of 5 s and all data were averaged to that time interval. The background signal was determined routinely in-flight by scrubbing NH_3 from the ambient sample and ranged from 0.5 to 1.3 ppbv. For a 5 s measurement the uncertainty in an individual background measurement varied from 20 to 60 pptv. The difference in consecutive background measurements ranged from 50 pptv to 100 pptv. Total uncertainty for the 5 s data was estimated at no worse than ±(30% + 125 pptv), though for certain individual flights it was less. The accuracy and precision of the airborne instrument was similar to the previous ground instruments [*Fehsenfeld et al.*, 2002; *Nowak et al.*, 2006]. However, the time response of the airborne instrument was faster and it was more sensitive than the instrument described by *Fehsenfeld et al.* [2002], primarily because of improvements in the ion transmission, inlet construction, and cleaner mass spectra due to use of a collisional dissociation chamber.

[27] The 5 s data obtained during NEAQS-ITCT enabled the observation of NH_3 from a variety of sources. Two plumes, one from an urban source and another from an agricultural one, are described here. During the 25 July flight, enhancements in NH_3 mixing ratios were coincident with enhancements in CO, NOx, and SO_2 mixing ratios downwind of New York City. The NH_3 mixing ratios in the urban outflow plume ranged from 0.4 to 1 ppbv. During the 15 August flight, NH_3 mixing ratios were enhanced directly downwind from an agricultural area northeast of Atlanta, Georgia. Here NH_3 mixing ratios ranged from 0.5 to 0.65 ppbv. In both cases, NH_3 mixing ratios decreased rapidly from the source. Whether this is due to surface deposition, loss to particles or clouds, or dilution due to plume dispersion has not been determined. However, given the number of sinks that can affect NH_3 mixing ratios it is clear that more observational data are needed to understand NH_3 transport and the regional impact of these sources.

[28] These results demonstrate that the airborne NH_3 CIMS instrument described here is selective, sensitive, and fast enough for use from aircraft platforms. Emission plumes with NH_3 mixing ratios of 0.4 ppbv or greater were easily distinguishable from the background air. However, there is room for improvement, particularly in determining the NH_3 mixing ratio in clean, remote air. The area in need of most improvement is understanding and controlling the background signal from the instrument. Both the absolute level and the variability in the background need to be reduced in order to measure ambient levels from 10 to 100 pptv. Possible improvements that show promise in postmission laboratory experiments are: the replacement of the N_2 cylinders used to supply the ion source flow with a cryogenic liquid N_2 source, a shorter flow tube reactor, the use of a higher purge flow between flights, and more diligence to prevent exposure of internal instrument parts to aircraft cabin air that had very high levels of NH_3. Nevertheless, these fast time resolution, sub-ppbv NH_3 measurements from an aircraft that have been used to identify NH_3 emissions from urban and agricultural sources.

[29] **Acknowledgments.** We thank the flight and support crew from the NOAA WP-3D aircraft for their efforts to make these measurements possible. The authors thank D. D. Parrish for helpful discussion and manuscript suggestions. Coauthors L. G. Huey and D. J. Tanner were supported by NOAA OGP grant NA04OAR43110088.

References

Alkezweeny, A. J., G. L. Laws, and W. Jones (1986), Aircraft and ground measurements of ammonia in Kentucky, *Atmos. Environ.*, *20*, 357–360.

ApSimon, H. M., et al. (1987), Ammonia emissions and their role in acid deposition, *Atmos. Environ.*, *21*, 1939–1946.

Ball, S. M., D. R. Hanson, F. L. Eisele, and P. H. McMurry (1999), Laboratory studies of particle nucleation: Initial results for H_2SO_4, H_2O, and NH_3 vapors, *J. Geophys. Res.*, *104*(D19), 23,709–23,718.

Clemitshaw, K. C. (2004), A review of instrumentation and measurement techniques for ground-based and airborne field studies of gas-phase tropospheric chemistry, *Crit. Rev. Environ. Sci. Technol.*, *34*, 1–108.

de Gouw, J. A., and C. Warneke (2006), Measurements of volatile organic compounds in the Earth's atmosphere using proton-transfer-reaction mass spectrometry, *Mass Spectrom. Rev.*, in press.

Dentener, F. J., and P. J. Crutzen (1994), A 3-dimensional model of the global ammonia cycle, *J. Atmos. Chem.*, *19*, 331–369.

Erisman, J. W., and M. Schaap (2004), The need for ammonia abatement with respect to secondary PM reductions in Europe, *Environ. Pollut.*, *129*, 159–163.

Fehsenfeld, F. C., L. G. Huey, E. Leibrock, R. Dissly, E. Williams, T. B. Ryerson, R. Norton, D. T. Sueper, and B. Hartsell (2002), Results from an informal intercomparison of ammonia measurement techniques, *J. Geophys. Res.*, *107*(D24), 4812, doi:10.1029/2001JD001327.

Fehsenfeld, F. C., et al. (2006), International Consortium for Atmospheric Research on Transport and Transformation (ICARTT): North America to Europe—Overview of the 2004 summer field study, *J. Geophys. Res.*, *111*, D23S01, doi:10.1029/2006JD007829.

Fraser, M. P., and G. R. Cass (1998), Detection of excess ammonia emissions from in-use vehicles and the implications for fine particle control, *Environ. Sci. Technol.*, *32*, 1053–1057.

Frost, G. J., et al. (2006), Effects of changing power plant NO_x emissions on ozone in the eastern United States: Proof of concept, *J. Geophys. Res.*, *111*, D12306, doi:10.1029/2005JD006354.

Gaydos, T. M., C. O. Stanier, and S. N. Pandis (2005), Modeling of in situ ultrafine atmospheric particle formation in the eastern United States, *J. Geophys. Res.*, *110*, D07S12, doi:10.1029/2004JD004683.

Goode, J. G., R. J. Yokelson, D. E. Ward, R. A. Susott, R. E. Babbitt, M. A. Davies, and W. M. Hao (2000), Measurements of excess O_3, CO_2, CH_4, C_2H_4, C_2H_2, HCN, NO, NH_3, HCOOH, CH_3COOH, HCHO, and CH_3H in 1997 Alaskan biomass burning plumes by airborne Fourier transform infrared spectroscopy, *J. Geophys. Res.*, *105*(D17), 22,147–22,166.

Hagg, C., and I. Szabo (1986), New ion-optical devices utilizing oscillatory electric-fields.2. Stability of ion motion in a two-dimensional hexapole field, *Int. J. Mass Spectrom. Ion Processes*, *73*, 237–275.

Hanson, D. R., and F. L. Eisele (2002), Measurement of prenucleation molecular clusters in the NH_3, H_2SO_4, H_2O system, *J. Geophys. Res.*, *107*(D12), 4158, doi:10.1029/2001JD001100.

Holloway, J. S., R. O. Jakoubek, D. D. Parrish, C. Gerbig, A. Volz-Thomas, S. Schmitgen, A. Fried, B. Wert, B. Henry, and J. R. Drummond (2000), Airborne intercomparison of vacuum ultraviolet fluorescence and tunable diode laser absorption measurements of tropospheric carbon monoxide, *J. Geophys. Res.*, *105*(D19), 24,251–24,261.

Huey, L. G. (2006), Measurement of trace atmospheric species by chemical ionization mass spectrometry: Speciation of reactive nitrogen and recent developments, *Mass Spectrom. Rev.*, in press.

Hurst, D. F., D. W. T. Griffith, J. N. Carras, D. J. Williams, and P. J. Fraser (1994), Measurements of trace gases emitted by Australian savanna fires during the 1990 dry season, *J. Atmos. Chem.*, *18*, 33–56.

Kean, A. J., R. A. Harley, D. Littlejohn, and G. R. Kendall (2000), On-road measurement of ammonia and other motor vehicle exhaust emissions, *Environ. Sci. Technol.*, *34*, 3535–3539.

LeBel, P. J., J. M. Hoell, J. S. Levine, and S. A. Vay (1985), Aircraft measurements of ammonia and nitric acid in the lower troposphere, *Geophys. Res. Lett.*, *12*, 401–404.

Li, Y., J. J. Schwab, and K. L. Demerjian (2006), Measurements of ambient ammonia using a tunable diode laser absorption spectrometer: Characteristics of ambient ammonia emissions in an urban area of New York City, *J. Geophys. Res.*, *111*, D10S02, doi:10.1029/2005JD006275.

McMurry, P. H., et al. (2005), A criterion for new particle formation in the sulfur-rich Atlanta atmosphere, *J. Geophys. Res.*, *110*, D22S02, doi:10.1029/2005JD005901.

Moeckli, M. A., M. Fierz, and M. W. Sigrist (1996), Emission factors for ethene and ammonia from a tunnel study with a photoacoustic trace gas detection system, *Environ. Sci. Technol.*, *30*, 2864–2867.

Neuman, J. A., L. G. Huey, T. B. Ryerson, and D. W. Fahey (1999), Study of inlet materials for sampling atmospheric nitric acid, *Environ. Sci. Technol.*, *33*, 1133–1136, doi:10.1021/es980767f.

Neuman, J. A., et al. (2002), Fast-response airborne in situ measurements of HNO_3 during the Texas 2000 Air Quality Study, *J. Geophys. Res.*, *107*(D20), 4436, doi:10.1029/2001JD001437.

Neuman, J. A., T. B. Ryerson, L. G. Huey, R. Jakoubek, J. B. Nowak, C. Simons, and F. C. Fehsenfeld (2003a), Calibration and evaluation of nitric acid and ammonia permeation tubes by UV optical absorption, *Environ. Sci. Technol.*, *37*, 2975–2981.

Neuman, J. A., et al. (2003b), Vertical gradients and spatial variability in ammonium nitrate formation and nitric acid depletion over California, *J. Geophys. Res.*, *108*(D17), 4557, doi:10.1029/2003JD003616.

Nowak, J. B., L. G. Huey, F. L. Eisele, D. J. Tanner, R. L. Mauldin III, C. Cantrell, E. Kosciuch, and D. D. Davis (2002), Chemical ionization mass spectrometry technique for detection of dimethylsulfoxide and ammonia, *J. Geophys. Res.*, *107*(D18), 4363, doi:10.1029/2001JD001058.

Nowak, J. B., et al. (2006), Analysis of urban gas phase ammonia measurements from the 2002 Atlanta Aerosol Nucleation and Real-Time Characterization Experiment (ANARChE), *J. Geophys. Res.*, *111*, D17308, doi:10.1029/2006JD007113.

Owens, M. A., C. C. Davis, and R. R. Dickerson (1999), A photothermal interferometer for gas-phase ammonia detection, *Anal. Chem.*, *71*(7), 1391–1399, doi:10.1021/ac980810h.

Perrino, C., M. Catrambone, A. Di Menno Di Bucchianico, and I. Allegrini (2002), Gaseous ammonia in the urban area of Rome, Italy and its relationship with traffic emissions, *Atmos. Environ.*, *36*, 5385–5394.

Ryerson, T. B., et al. (1998), Emissions lifetime and ozone formation in power plant plumes, *J. Geophys. Res.*, *103*(D17), 22,569–22,583.

Ryerson, T. B., L. G. Huey, K. Knapp, J. A. Neuman, D. D. Parrish, D. T. Sueper, and F. C. Fehsenfeld (1999), Design and initial characterization of an inlet for gas-phase NO_y measurements from aircraft, *J. Geophys. Res.*, *104*(D5), 5483–5492.

Ryerson, T. B., E. J. Williams, and F. C. Fehsenfeld (2000), An efficient photolysis system for fast-response NO_2 measurements, *J. Geophys. Res.*, *105*(D21), 26,447–26,462.

Schlesinger, W. H., and A. E. Hartley (1992), A global budget for atmospheric NH_3, *Biogeochemistry*, *15*, 191–211.

Sinha, P., P. V. Hobbs, R. J. Yokelson, I. T. Bertschi, D. R. Blake, I. J. Simpson, S. Gao, T. W. Kirchstetter, and T. Novakov (2003), Emissions of trace gases and particles from savanna fires in southern Africa, *J. Geophys. Res.*, *108*(D13), 8487, doi:10.1029/2002JD002325.

Slusher, D. L., L. G. Huey, D. J. Tanner, F. M. Flocke, and J. M. Roberts (2004), A thermal dissociation–chemical ionization mass spectrometry (TD-CIMS) technique for the simultaneous measurement of peroxyacyl nitrates and dinitrogen pentoxide, *J. Geophys. Res.*, *109*, D19315, doi:10.1029/2004JD004670.

Talbot, R. W., et al. (1997), Chemical characteristics of continental outflow from Asia to the troposphere over the western Pacific Ocean during February–March 1994: Results from PEM-West B, *J. Geophys. Res.*, *102*(D23), 28,255–28,274.

Tanner, D. J., A. Jefferson, and F. L. Eisele (1997), Selected ion chemical ionization mass spectrometric measurement of OH, *J. Geophys. Res.*, *102*(D5), 6415–6426.

Weber, R. J., P. H. McMurry, L. Mauldin, D. J. Tanner, F. L. Eisele, F. J. Brechtel, S. M. Kreidenweis, G. L. Kok, R. D. Schillawski, and D. Baumgardner (1998), A study of new particle formation and growth involving biogenic and trace gas species measured during ACE 1, *J. Geophys. Res.*, *103*(D13), 16,385–16,396.

Yokelson, R. J., J. G. Goode, D. E. Ward, R. A. Susott, R. E. Babbitt, D. D. Wade, I. Bertschi, D. W. T. Griffith, and W. M. Hao (1999), Emissions of formaldehyde, acetic acid, methanol, and other trace gases from biomass fires in North Carolina measured by airborne Fourier transform infrared spectroscopy, *J. Geophys. Res.*, *104*(D23), 30,109–30,126.

Yokelson, R. J., I. T. Bertschi, T. J. Christian, P. V. Hobbs, D. E. Ward, and W. M. Hao (2003a), Trace gas measurements in nascent, aged, and cloud-processed smoke from African savanna fires by airborne Fourier transform infrared spectroscopy (AFTIR), *J. Geophys. Res.*, *108*(D13), 8478, doi:10.1029/2002JD002322.

Yokelson, R. J., T. J. Christian, I. T. Bertschi, and W. M. Hao (2003b), Evaluation of adsorption effects on measurements of ammonia, acetic acid, and methanol, *J. Geophys. Res.*, *108*(D20), 4649, doi:10.1029/2003JD003549.

F. C. Fehsenfeld and T. B. Ryerson, Chemical Sciences Division, Earth System Research Laboratory, NOAA, Boulder, CO 80305, USA.

G. J. Frost, J. S. Holloway, S. A. McKeen, J. A. Neuman, and J. B. Nowak, Cooperative Institute for Research in Environmental Sciences, University of Colorado, Boulder, CO 80309, USA.

L. G. Huey and D. J. Tanner, School of Earth and Atmospheric Sciences, Georgia Institute of Technology, Atlanta, GA 30332, USA.

K. Kozai, Department of Mathematics, Harvey Mudd College, Claremont, CA 91711, USA.